J. Chem. Sci., Vol. 118, No. 1, January 2006, pp. 105–115.

Inclusion of poly-aromatic hydrocarbon (PAH) molecules in a functionalized layered double hydroxide

L MOHANAMBE and S VASUDEVAN*

Department of Inorganic and Physical Chemistry, Indian Institute of Science, Bangalore 560 012
e-mail: svipc@ipc.iisc.ernet.in

Abstract. The internal surface of an Mg–Al layered double hydroxide has been functionalized by anchoring carboxy-methyl derivatized *b*-cyclodextrin cavities to the gallery walls. Neutral polyaromatic hydrocarbon (PAH) molecules have been included within the functionalized solid by driving the hydrophobic aromatic molecules from a polar solvent into the less polar interior of the anchored cyclodextrin cavities by a partitioning process. The optical (absorption and emission) properties of the PAH molecules included within the functionalized Mg–Al layered double hydroxide solid are similar to that of dilute solutions of the PAH in non-polar solvents. The unique feature of these hybrid materials is that they are thermally stable over a wide temperature range with their emission properties practically unaltered.

Keywords. Layered double hydroxide; polyaromatic hydrocarbon molecules; thermal; emission properties.

1. Introduction

Inorganic layered solids in which guest species can access interlamellar space via the intercalation reaction offer a unique route to the design of new hybrids that combine the functionality and properties of host and guest at the molecular level. In a majority of these solids, intercalation is driven either by oxidation–reduction, acid–base or ion-exchange reactions. The interaction between host and guest is coulombic, with the guest species compensating for the charge deficit, either positive or negative, of the inorganic layer. Typical examples of these solids are the phyllosilicate clays, the layered double hydroxides, the divalent metal thiophosphates and metal (IV) phosphates and phosphonates.[1,2] The subsequent host–guest chemistry of these intercalated solids is restricted to exchange of the interlamellar charged species for other ions and, to a limited extent, adsorption of polar molecules, e.g. crown ethers[3] and polyethylene oxide,[4,5] through ion-dipole interactions. It is, therefore, not possible to directly insert, by intercalation, neutral non-polar molecules e.g. poly-nuclear aromatic hydrocarbons (PAH), within these layered inorganic solids.

The host-guest chemistry of these solids can, however, is extended to include non-polar and poorly water-soluble molecules by appropriate functionalization of the internal surface of the solid. Anchoring of long chain surfactant molecules to the walls of the galleries is one of the well-established strategies to solubilize neutral organic molecules within an inorganic solid.[6–9] Certain structural arrangements of the anchored surfactant, like the intercalated bilayer can, in fact, act as membrane mimics allowing for the incorporation of bio-molecules like cholesterol within the hydrophobic interior of the bilayer.[10]

Host structures are, of course, not limited to inorganic solids, a variety of organic hosts are known, the most well known of which are the crown ethers, cyclodextrins, calixarenes and spherands.[11] These molecules, which are soluble in aqueous and organic solvents, can act as hosts for a variety of neutral organic molecules. In principle, if the two host structures, the layered inorganic solid and the organic host, can be integrated, a new family of host structure can be envisaged. Indeed, such organic–inorganic hybrid structures have been realized; modified cyclodextrins have been successfully intercalated in montmorillonite clays,[12] zirconium phosphates[13] and layered double hydroxides[14,15] to create a new generation of host structures. Cyclodextrins, herein abbreviated as CDs, are cyclic oligomers of *d*-glucopyranose ($C_6H_{10}O$) with cylindrical hydrophobic cavities into which a variety of small molecules may be introduced. The solubilization of hydrophobic molecules like aromatic hydrocarbons in aqueous media by cyclodex-

Dedicated to Prof J Gopalakrishnan on his 62nd birthday
*For correspondence

trins is well known and have been extensively studied.[16] For PAH molecules with *b*-cyclodextrin, the commonly encountered stoichiometry is the 1 : 1 complex although other stoichiometries like 2 : 2 have also been reported for naphthalene and pyrene.[17]

Layered double hydroxides (LDH), the so-called anionic clays, consists of positively charged brucite-like layers and interlamellar exchangeable anions.[18] Hydrotalcites are layered double hydroxides with the chemical composition $[Mg_{1-x}Al_x(OH)_2]^{x+}[A^n]_{x/n}.mH_2O$ (Mg–Al–LDH) that consist of positively charged layers constructed from edge sharing $Mg(OH)_6$ and $Al(OH)_6$ octahedra.[19–22] The positive charge of the layers is compensated for by interlayer anions that are usually hydrated and can be exchanged for other inorganic or organic anions. They have been used as catalysts and catalyst precursors, sorbents and scavengers for halogens and weak acids[23–27] and more recently for storing and delivering biologically active materials.[28,29] The guest species, however, have, of necessity, to be anions for charge neutrality to be preserved and as a consequence, the host–guest chemistry of the LDH's is limited to ion-exchange reactions. However, when the internal surface of an Mg–Al LDH is functionalized by anchoring *b*-cyclodextrin cavities to the gallery walls (figure 1), it is possible to insert neutral organometallic[30] and aromatic hydrocarbon[31,32] molecules within the inorganic solid as well as adsorb iodine from vapour as well as from non-polar solvents.[33] Insertion occurs by the inclusion of the non-polar guest molecules within the hydrophobic interior of the anchored cyclodextrin cavities. We show here that this novel hybrid combines the functionality of the organic guest with the mechanical and thermal robustness of the inorganic solid.

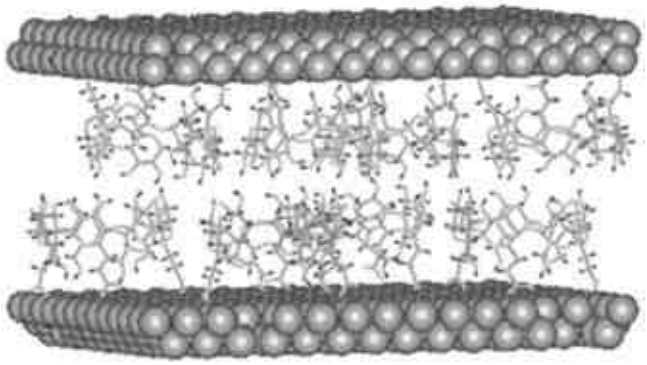

Figure 1. A model representing the arrangement of CMCD molecules within the galleries of Mg–Al LDH.

2. Experimental

2.1 *Preparation and characterization*

$Mg_{1-x}Al_x(OH)_2(NO_3)_x$ [Mg–Al LDH-NO_3] was prepared by co-precipitation, by dropwise addition of known volumes of aqueous $Mg(NO_3)_2$ (0·04 M) and $Al(NO_3)_3$ (0·02 M) into NaOH solution at a constant pH of 8, under N_2 atmosphere, following the procedure reported by Meyn *et al*.[34] The resulting white precipitate was aged for 24 h prior to washing with de-carbonated water. The anchoring of *b*-cyclodextrin cavities within the Mg–Al LDH was achieved by ion-exchanging the NO_3 ions in $Mg_{1-x}Al_x(OH)_2(NO_3)_x$ with methylcarboxylate derivatized *b*-cyclodextrin anions. The sodium salt of carboxymethyl *b*-cyclodextrin, $C_{42}H_{70-n}O_{35}(CH_3COONa)_n$ (CMCD) was obtained from Cerestar Company (Hammond, In, USA). The average number of carboxylate groups per *b*-CMCD molecule, as established by pH titrations, is 3·8.

The ion-exchange intercalation of *b*-CMCD in the LDH was effected following the procedure of ref. [15]. Mg–Al LDH-NO_3 (100 mg) was added to 10 ml of 10 mM of aqueous *b*-CMCD solution at 65°C and stirred for 24 h. Completion of the intercalation of the *b*-CMCD was confirmed by the absence of 00*l* reflections with a basal spacing of 8·9 Å and the appearance of a new set of 00*l* reflections with a basal spacing of 24·5 Å as determined from the powder X-ray diffraction patterns. The *b*-CMCD stoichiometry in the LDH was established from CHN elemental analysis (C% = 18·9, H% = 5·06) and also from the concentration of the un-exchanged *b*-CMCD remaining in the reactant solution. Mg/Al ratios in the LDH were determined by inductively coupled plasma spectroscopy (Jobin Yvon JY24). The composition of the starting Mg–Al LDH-NO_3 was $Mg_{0·7}Al_{0·3}(OH)_2(NO_3)_{0·3}$ and of Mg–Al LDH-CMCD was $Mg_{0·7}Al_{0·3}(OH)_2(CMCD)_{0·073}$.

Benzene, naphthalene, anthracene, pyrene and phenanthrene were the poly-aromatic hydrocarbons (PAHs) inserted as guest molecules in the functionalized Mg–Al LDH-CMCD. Inclusion was effected by sorption from either a saturated aqueous solution or a methanol-water solution of the PAH. In a typical sorption experiment, 2 mg of Mg–Al LDH-CMCD was allowed to equilibrate with 10 ml of aqueous PAH solution of known concentration for a period of 3 days at room temperature. Adsorption isotherms for the inclusion of naphthalene were obtained by

determining the concentration of included naphthalene as the difference in the concentration of naphthalene in the aqueous (or methanol–water) solution before and after equilibration. The concentration of naphthalene in solution was obtained by monitoring the absorbance at $l \sim 276$ nm by UV–visible spectroscopy.

2.2 *Measurement techniques*

Powder X-ray diffraction patterns of Mg–Al LDH-NO_3, Mg–Al LDH-CMCD and Mg–Al LDH-CMCD (PAH) were recorded on a Shimadzu XD-D1 X-ray diffractometer using CuK_a radiation of l 1·54 Å. The samples were mounted by pressing the powders on a glass plate and the data were collected at a scan speed of 2° 2q/min. CHN analysis was performed on a CHNS (CARLO ERBA) elemental analyzer. FT-IR spectra were recorded as KBr pellets on a Bruker IFS55 spectrometer operating at 4 cm^{-1} resolution. FT-Raman spectra were recorded on a Bruker IFS FT-Raman spectrometer using an Nd:YAG (l = 1·064 nm) laser for excitation. Spectra were recorded at a resolution of 4 cm^{-1} with an unpolarised beam using an Al sample holder. Laser power was kept at 150 mw. Fluorescence spectra were recorded on a Perkin–Elmer LS50B model, with excitation and emission slit-widths of 5–10 nm and a scan speed of 60 nm/min. For variable temperature measurements, a CTI-Cryogenics closed cycle cryostat was used. Sample temperatures could be varied from 40 to 500 K. TGA was recorded on a Perkin–Elmer–Pyris–Diamond thermo gravimetric/differential thermal analyzer (TG/DTA) system in flowing air.

3. Results

3.1 *Carboxymethyl b-cyclodextrin functionalized Mg–Al LDH*

The ion-exchange intercalation of *b*-CMCD, with an average degree of carboxymethyl substitutions of 3·8 per cyclodextrin molecule, in $Mg_{0·7}Al_{0·3}(OH)_2(NO_3)_{0·3}$ occurs with an increase in the interlayer lattice spacing from 8·9 Å to 24·6 Å (figure 2a) that corresponds to a lattice expansion of 19·8 Å.[15] The intercalated Mg–Al LDH-CMCD is stable on exposure to the atmosphere as well as moisture and the anchored *b*-CMCDs are no longer exchangeable, e.g. with carbonate ions. Thermo-gravimetric analysis (TGA) of Mg–Al LDH-CMCD (figure 3) shows a two-step weight loss. There is a ~8%, weight loss at ~80°C that probably corresponds to water sticking to the exterior of the crystallites and a gradual weight loss (~7%) between 80°C and 250°C possibly be due to interlamellar water. The second weight loss at ~300°C is due to the decomposition of the intercalated carboxymethyl *b*-cyclodextrin. The Na salt of CMCD decomposes at 270°C.

The ^{13}C CP-MAS NMR of the Mg–Al LDH-CMCD and that of the sodium salt of *b*-CMCD are shown in figure 2b along with the assignments for the resonances. The positions of the resonances in the two compounds are identical indicating that the integrity of the cyclodextrin cavity is preserved on intercalation. This was further confirmed by the fact that the positions of the infrared and Raman bands of the two compounds were identical (figure 4). To summarize, the NMR and vibrational spectra indicate that the structural integrity of the *b*-cyclodextrin cavity is preserved on intercalation in the Mg–Al LDH. The absence of any significant change in the positions of the vibrational modes of the glucopyranose units as well as in their linkages in the infrared and Raman spectra suggests that the geometry of the intercalated *b*-cyclodextrin cavity is essentially the same as that outside the layers.

The observed lattice expansion and stoichiometry can be accounted for by a perpendicular bilayer arrangement of the cyclodextrin molecules in the galleries, with the axis of the cyclodextrin cavities parallel to the interlayer normal.[15] The *b*-cyclodextrin molecule may be considered a truncated cone with an approximate torus thickness of 7·8 Å. The outer diameter of the wider end of the cone is 15·4 Å while that of the narrower end is 7·8 Å. The carboxymethyl groups are attached by substitution of the primary hydroxyl groups located at the narrower end of the truncated cone.[11] Molecular modelling shows that the presence of the carboxymethyl groups increases the effective torus thickness by 1·46 Å. The perpendicular bilayer arrangement would therefore result in an interlayer expansion of 18·52 Å, which is close to the experimental value of 19·8 Å.

3.2 *Polarity of the anchored carboxymethyl-b-cyclodextrin*

In order to establish the hydrophobicity of the microenvironment within the anchored cyclodextrin cavities, the fluorescence spectra of pyrene included within the Mg–Al LDH-CMCD was examined. The

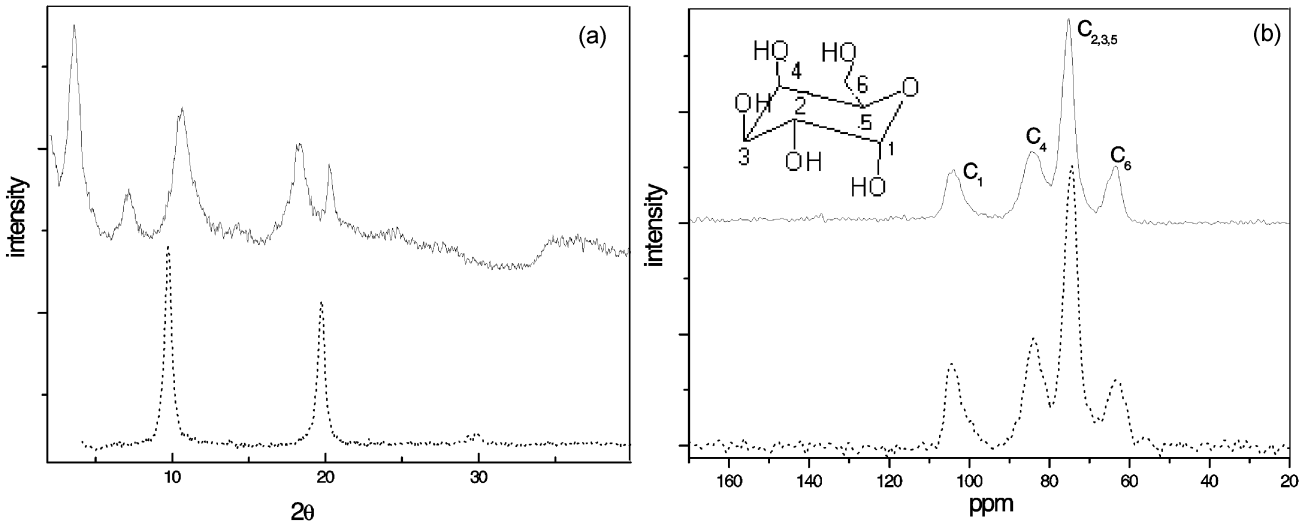

Figure 2. (**a**) X-ray diffraction pattern and (**b**) ^{13}C CP-MAS NMR of Mg–Al LDH-CMCD and Mg–Al LDH-NO_3 (dotted line).

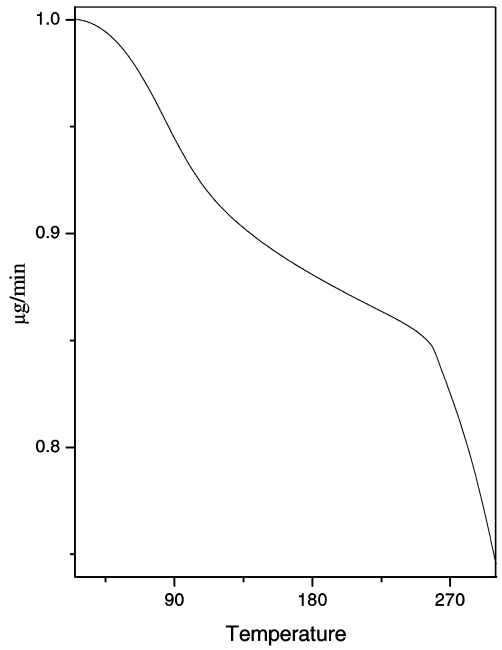

Figure 3. Thermo-gravimetric analysis of Mg–Al LDH-CMCD.

fluorescence of pyrene has been widely used to establish the polarity of the medium in which it is present.[35] In polar solvents, there is an enhancement in the intensity of the symmetry forbidden (0–0) band (Ham effect).[36] The relative intensity of the first, I_I, and third, I_{III}, vibronic bands of the first singlet emission ($S_1 \rightarrow S_0$) correlates reasonably well with solvent polarity. The intensity ratio of pyrene, I_I/I_{III}, varies, typically, from 0·6 in non-polar solvents, like hexane, to 1·95 in polar solvents like dimethyl sulphoxide.[37]

The fluorescence spectrum of pyrene included within the Mg–Al LDH-CMCD by sorption from an aqueous solution (~0·8 *m*M) of pyrene is shown as an inset in figure 5. The emission spectra were obtained by excitation within the pyrene absorption band at 335 nm. The average value of the intensity ratio of I_I/I_{III} ($I_{370\ nm}/I_{390\ nm}$) is 0·92. In order to place this value on a relative polarity scale, the fluorescence spectra of pyrene in different solvents were recorded and the values of the intensity ratio of I_I/I_{III} plotted as a function of the dielectric constant of the solvent (figure 5). It may be seen from figure 5 that the polarity within the cavities of the anchored cyclodextrins lie in between that of methanol and 1:1 methanol–water mixture. The value of the dielectric constant ~55 is similar to that reported for *b*-cyclodextrin cavities.[17] The data of figure 5 suggest that it may be possible to drive a hydrophobic guest molecules into anchored cyclodextrin cavities from polar solvents, those that lie to the right of the Mg–Al LDH-CMCD in figure 5.

3.3 *Partitioning equilibria*

The poly-aromatic hydrocarbons naphthalene,[31] anthracene,[32] pyrene and phenenathrene, as well as benzene (for reference) were partitioned into the Mg–Al LDH-CMCD from aqueous solutions. The inclusion of the PAHs in the Mg–Al LDH-CMCD

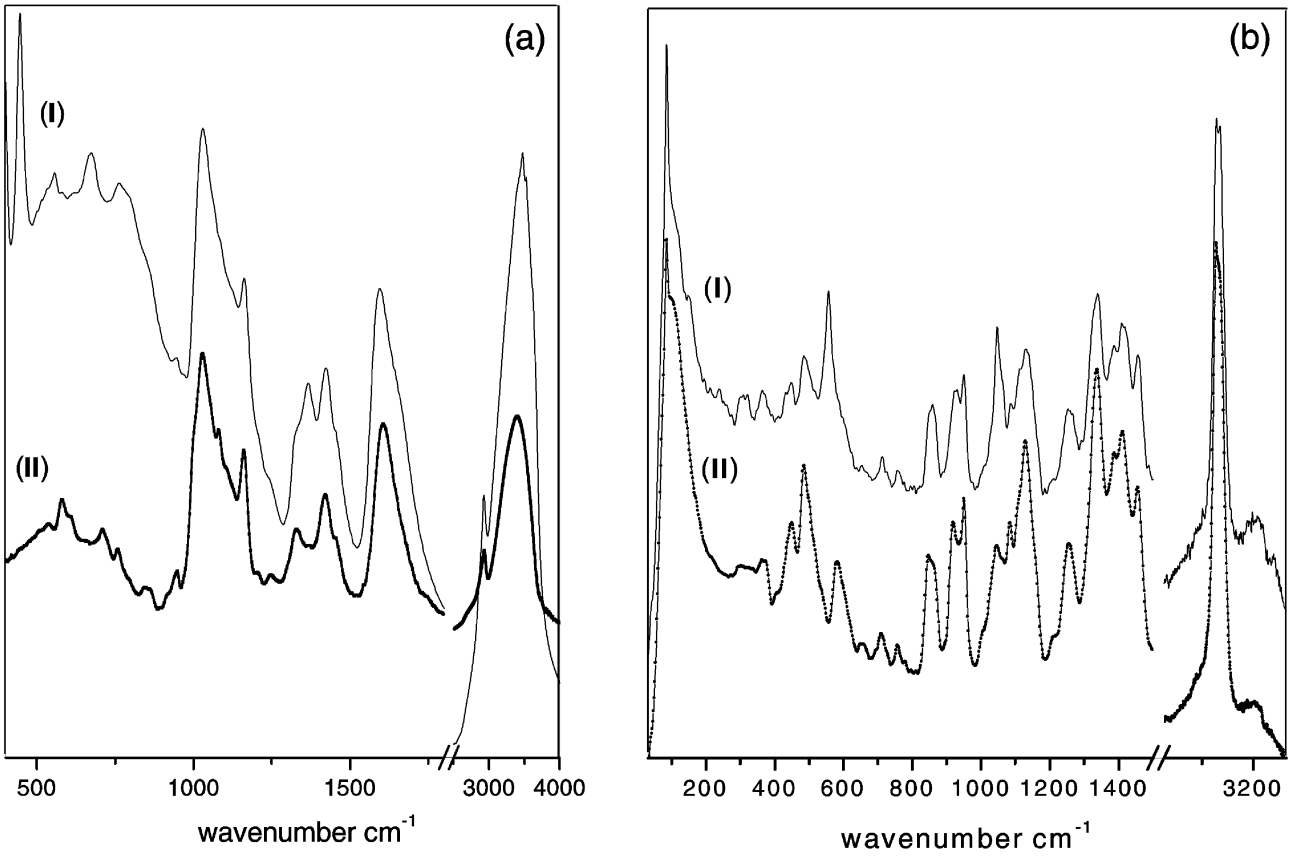

Figure 4. (**a**) Infrared spectra and (**b**) Raman spectra of (I) Mg–Al LDH-CMCD and (II) Na salt of CMCD.

does not lead to any change in the inter-layer spacing; the X-ray diffraction patterns were identical to that in figure 2a. Insertion of PAHs does not lead to any change in the composition of the host Mg–Al LDH-CMCD. Thermo-gravimetric measurements showed that the PAH inclusion compounds were thermally stable up to 550 K at which temperature the parent Mg–Al LDH-CMCD decomposes. The position of the infrared and Raman vibrational modes of the intercalated cyclodextrin also show no change on inclusion of PAHs. The Raman spectra, however, show additional bands of the included PAH (figure 6 and table 1). The fact that the vibrational bands of the intercalated cyclodextrin show no significant change suggests that they may be considered as rigid hydrophobic containers for the inclusion of the PAHs.

The equilibrium uptake of naphthalene by the Mg–Al LDH-CMCD from aqueous as well as solutions in three different methanol–water mixtures of differing polarity is shown in figure 7. The amount of naphthalene included in the Mg–Al LDH-CMCD, expressed as the molar ratio of included naphthalene to anchored cyclodextrin cavities in the LDH (referred to as the naphthalene/CMCD mol ratio), is plotted as a function of the molar concentration of the naphthalene solution in figure 7. The adsorption isotherms are linear with the slope proportional to the polarity of the solution. The maximum uptake is from aqueous solutions while there is practically no uptake from the 2:1 methanol–water solution, the least polar of the four solvents. The linearity of the isotherms is consistent with the idea that the sorption of naphthalene by the Mg–Al LDH-CMCD is a partitioning process rather than physical adsorption.[38] The slope of the isotherm, the partition coefficient, clearly indicates that the partitioning equilibria favours the less polar environment for the hydrophobic ‘solute’, naphthalene.

3.4 *Optical properties*

The photo-physics and luminescence of poly-aromatic hydrocarbons are one of their most significant and widely studied properties.[39] We have examined

Table 1. Raman spectral positions and assignments of naphthalene (solid), LDH-CMCD, LDH-CMCD (naphthalene)$_{0.45}$ at room temperature and at 373 K.

Naphthalene (solid) cm^{-1}	LDH-CMCD (naphthalene) (cm^{-1}) 273 K	LDH-CMCD (naphthalene) (cm^{-1}) 373 K	LDH-CMCD	Assignment
3056	3056 (br)	3056 (br)	–	Sym. C–H stretch
–	2915 (br)	2915 (br)	2915 (br)	C–H stretch
1577 (br)	1577 (br)	1577 (br)	–	Sym. C–C stretch
1444	1438 (weak)	1436 (br)	–	Sym. C–H bending
	1407, 1333	1407, 1333	1410 (br), 1338	C–C stretch, C–O–H bond, CH_2 deformation
1382	1379	1377	–	Asym. C–C stretch
	1255, 1130, 1043	1255, 1130, 1038	1255, 1130, 1048	C–O–H stretch, OH deformation, C–C skeletal stretch
1020	1024	1024	–	Sym. C–C stretch
–	949, 924	924 (broad)	949, 924	C–O–C stretch of (1 4) linkages
763	760	759	–	Skeletal sym. breathing
	552	555	556	CMCD-ring vibrations
513	510	510	–	Skeletal distortion
392	392 (weak, br)	392	–	Skeletal bending

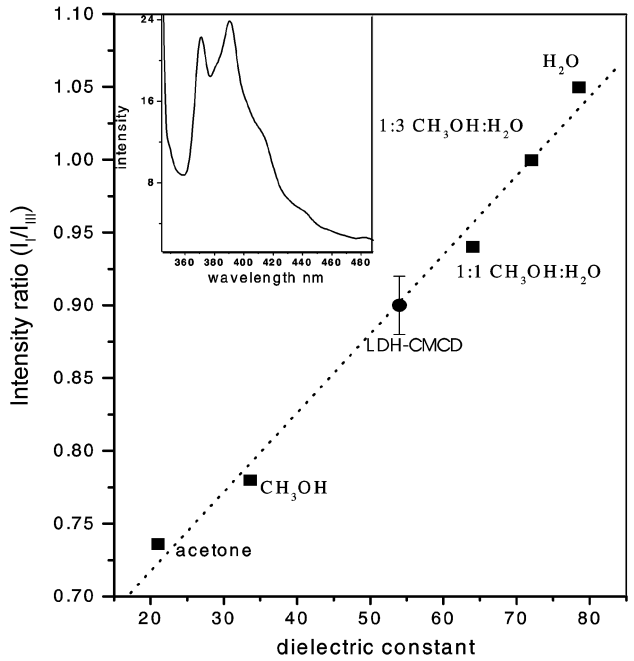

Figure 5. The variation of the intensity ratio of the first and third vibronic bands in the fluorescence spectra of pyrene, I_I/I_{III}, as function of solvent polarity. The bar indicates the range of I_I/I_{III} ratios observed for pyrene included within Mg–Al LDH-CMCD. The inset shows the fluorescence spectra of pyrene included within Mg–Al LDH-CMCD.

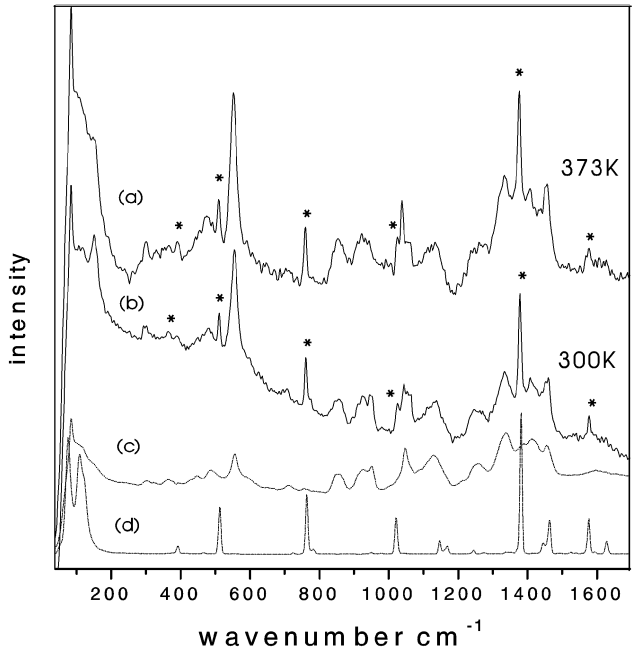

Figure 6. Raman spectra of Mg–Al LDH-CMCD (naphthalene) at (a) 300 K and (b) 373 K. The bands due to the included naphthalene are indicated. For comparison the spectra of (c) Mg–Al LDH-CMCD and (d) naphthalene solid are also shown.

the optical – absorption and fluorescence – spectra of these aromatic molecules included within the anchored cyclodextrin cavities of the Mg–Al LDH-CMCD. The room temperature fluorescence excitation and emission spectra of naphthalene, anthracene, pyrene and phenanthrene included in the functionalized LDH are shown in figures 8a–d and the band positions and assignments tabulated in table 2. In all the systems studied, the spectra are highly structured with the vibronic bands reasonably well resolved. The quality and resolution of features in the spectra, recorded in the solid state (figure 8), are comparable to the reported spectra of dilute solutions of the PAHs in non-polar solvents.[39] The absorption and excitation spectra are similar but features are less resolved in the former due to spectral broadening.

The fluorescence excitation and emission spectra of naphthalene included in Mg–Al LDH-CMCD are shown in figure 8a. The spectral features at 222 and 287 nm in the excitation spectra are due to the $S_0 \rightarrow S_3$ and $S_0 \rightarrow S_2$ transitions respectively, while the bands at 267 and 276 nm are the vibronic states associated with the $S_0 \rightarrow S_2$ transition. The weak absorptions at 300 and 310 nm are transitions from the ground state to the first excited state ($S_0 \rightarrow S_1$). The corresponding emission ($S_1 \rightarrow S_0$) in the fluorescence spectra appears at 322 (0–0), 332 (1–0) and 346 (2–0) nm. The positions of the bands in both the excitation and emission spectra of the Mg–Al LDH-CMCD(naphthalene) are identical to those for dilute solutions of naphthalene in hexane.[39]

The excitation spectra of anthracene in the Mg–Al LDH-CMCD shows the $S_0 \rightarrow S_2$ and $S_0 \rightarrow S_1$ transition at 252 and 377 nm, respectively with the vibronic structure being well resolved for the latter (Figure 8b). The corresponding $S_1 \rightarrow S_0$ emission (370–450 nm), too, shows clearly resolved transitions associated with the vibronic states. The emission band at 300 nm is probably due to the $S_2 \rightarrow S_0$ transition. As in the case of the included naphthalene, the positions of the bands in the excitation and emission spectra are identical to those of a dilute solution of anthracene in hexane.

The excitation and emission spectra of pyrene included within the Mg–Al LDH-CMCD are shown in figure 8c. The spectra are similar to that of pyrene in dilute solutions and also to that of isolated pyrene-*b*-

Table 2. Fluorescence excitation and emission spectral band positions and their assignments of Mg–Al LDH-CMCD(PAH).

Sample	Excitation spectra (nm)	Emission spectra (nm)	Assignments
LDH-CMCD	300		*S*0–*S*1
(naphthalene)	310		(0–0)
	267		*S*0–*S*2
	276		
	287		(0–0)
	222		*S*0–*S*3 (0–0)
		322	*S*1–*S*0
		332	
		346	(0–0)
LDH-CMCD	377		*S*0–*S*1 (0–0)
(anthracene)			
	252		*S*0–*S*2 (0–0)
		377	*S*1–*S*0 (0–0)
		399	
		421	
		300	*S*2–*S*0
LDH-CMCD	337		*S*0–*S*2 (0–0)
(pyrene)	322		
	272		*S*0–*S*3 (0–0)
	239		*S*0–*S*4 (0–0)
		370	*S*1–*S*0 (0–0)
		384	
		390	
LDH-CMCD	294		*S*0–*S*2 (0–0)
(phenanthrene)	254		*S*0–*S*3 (0–0)
		348	*S*1–*S*0 (0–0)
		363	
		378	

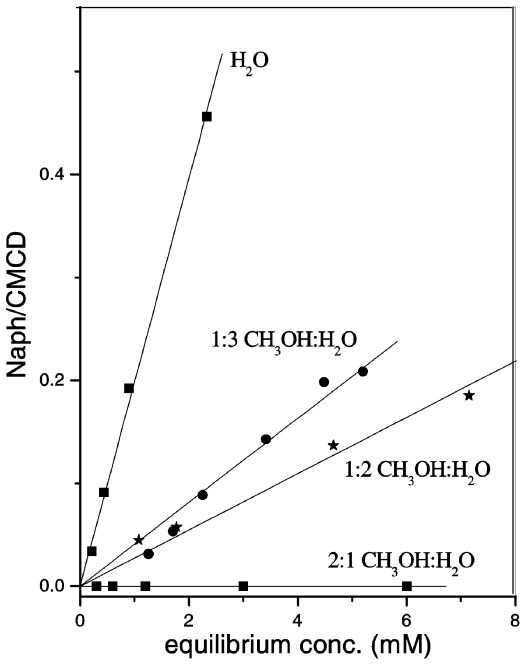

Figure 7. Equilibrium uptake of naphthalene by Mg–Al LDH-CMCD at 298 K from different methanol-water mixture solutions.

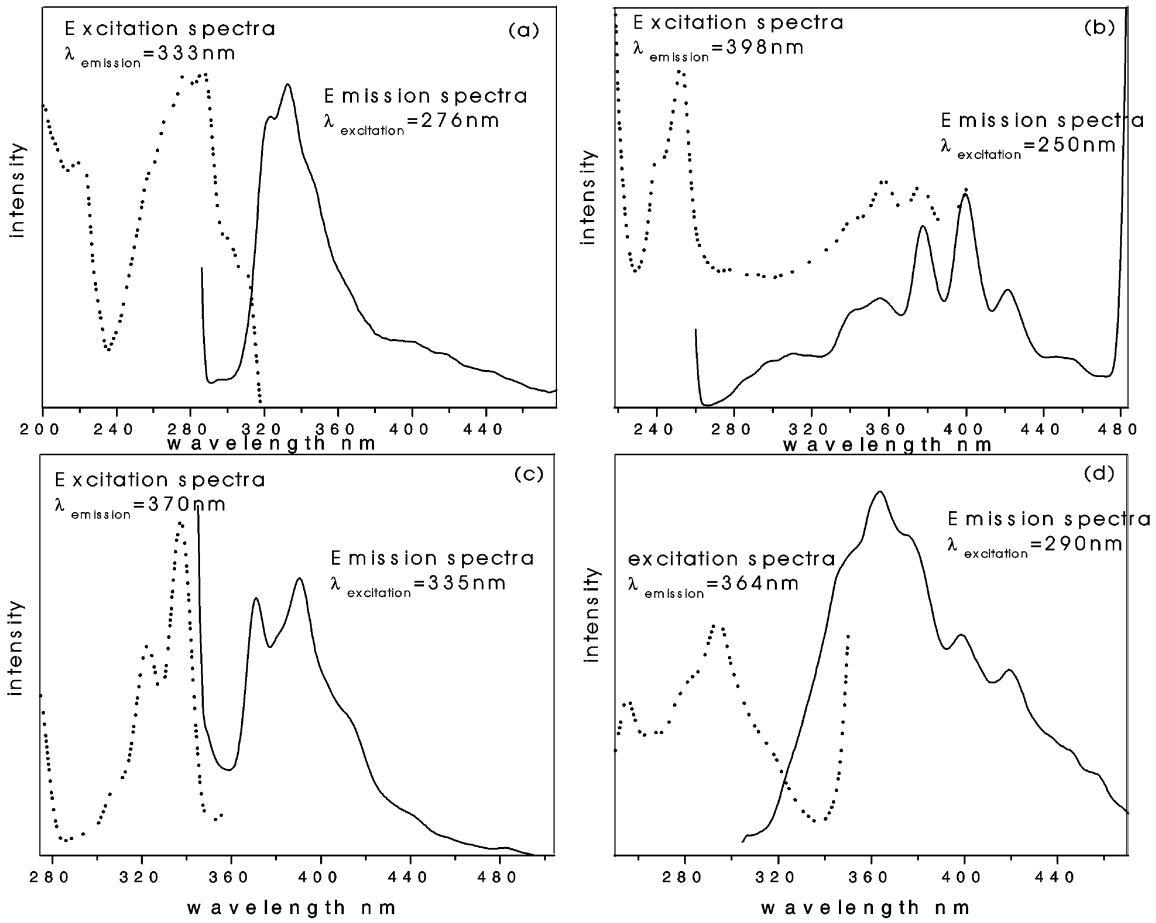

Figure 8. Excitation and emission spectra of (**a**) Mg–Al LDH-CMCD (naphthalene), (**b**) Mg–Al LDH-CMCD (anthracene), (**c**) Mg–Al LDH-CMCD (pyrene) and (**d**) Mg–Al LDH-CMCD (phenanthrene). The emission wavelength at which the excitation spectra were recorded and the excitation wavelength at which the emission spectra were recorded is indicated on each panel.

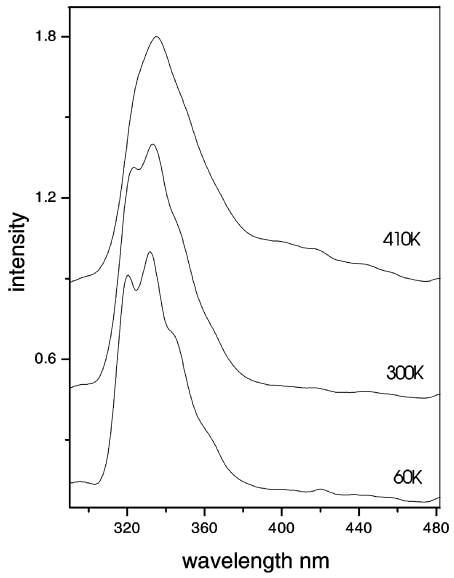

Figure 9. Fluorescence emission spectra of Mg–Al LDH-CMCD (naphthalene) at different temperatures.

CD complexes trapped in sol–gel glasses.[40] The features at 272 and 337 nm in the excitation spectra are the $S_0 \rightarrow S_3$ and $S_0 \rightarrow S_2$ transitions respectively while the shoulder at 239 nm is the $S_0 \rightarrow S_4$ excitation. As expected, the symmetry forbidden $S_0 \rightarrow S_1$ band is absent in the spectrum of the included pyrene. The symmetry selection rules also apply for phenanthrene included in the Mg–Al LDH-CMCD; the $S_0 \rightarrow S_1$ is absent in the excitation spectra, while in the fluorescence spectrum, the transitions involving the higher vibrational states of the $S_1 \rightarrow S_0$ emission are prominent (figure 8d). The $S_1 \rightarrow S_0$ (0–0) transition is the shoulder at 347 nm in the fluorescence spectrum.

3.5 *Thermal stability*

The fluorescence spectra of the naphthalene included within the cyclodextrin functionalized LDH

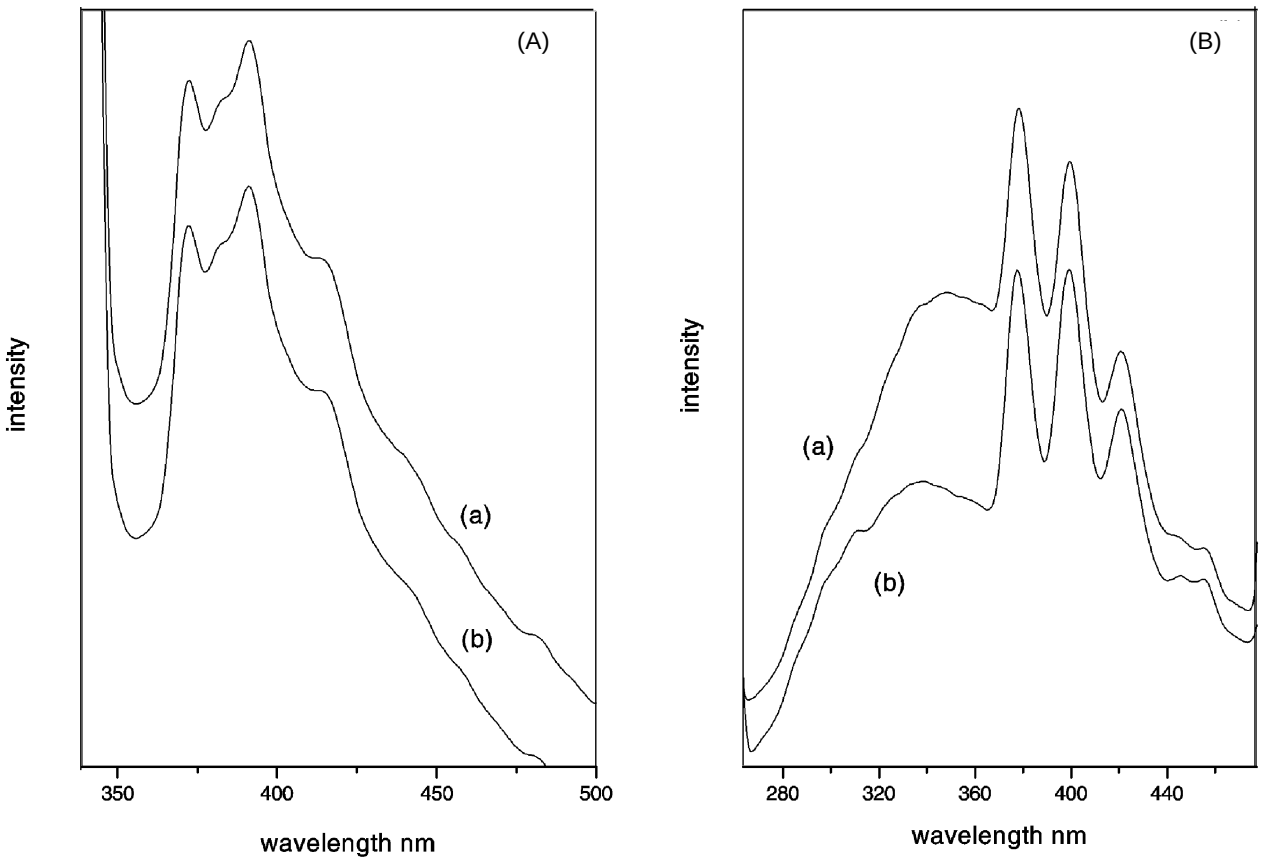

Figure 10. Emission spectra of (**A**) Mg–Al LDH-CMCD (pyrene) and (**B**) Mg–Al LDH-CMCD (anthracene) at room temperature before (a) and after (b) heating to 500 K.

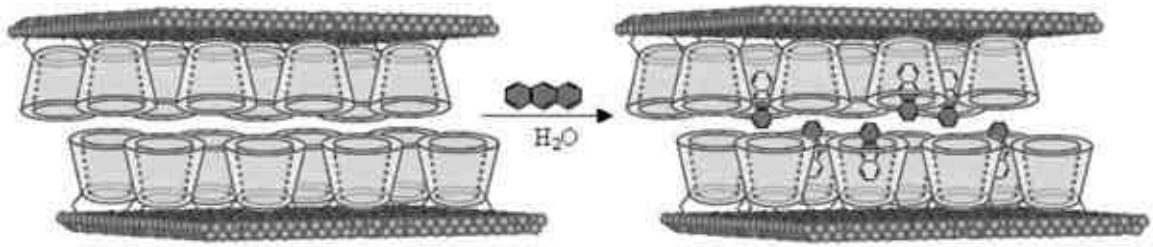

Figure 11. Cartoon illustrating the inclusion of a PAH anthracene, within the anchored cyclodextrin cavities by partitioning from a polar solvent.

solid, recorded at different temperatures is shown in figure 9. The emission corresponds to the $S_1 \rightarrow S_0$ transition. The unique feature of these hybrid materials is that they are thermally stable over a wide temperature range with their emission properties practically unaltered. It may be seen that apart from changes in the relative intensities of the vibronic transitions arising from changes in the Boltzman distribution at different temperatures, the spectra are similar. The thermal robustness of these materials is clearly demonstrated from the fact that we are able to observe the emission spectra even at temperatures above those at which naphthalene solid would normally sublime (~353 K). The 410 K fluorescence spectra of the Mg–Al LDH-CMCD (naphthalene) clearly eliminate the possibility that the observed optical properties are due to naphthalene sticking to the exterior of the Mg–Al LDH-CMCD crystallites.

The behaviour of the other Mg–Al LDH-CMCD (PAH)s are similar with the emission spectra remaining essentially unaltered at elevated temperatures. The Mg–Al LDH-CMCD(PAH) can, in fact, be heated to temperatures close to the decomposition temperature (550 K); cooled back to room temperature and the fluorescence spectra reproduced (figure 10).

Conclusions

The internal surface of an Mg–Al layered double hydroxide has been functionalized by anchoring carboxymethyl derivatized *b*-cyclodextrin cavities to the gallery walls. The structural integrity of the cyclodextrin cavity is preserved on intercalation. The fluorescence spectra of pyrene included within the functionalized Mg–Al LDH-CMCD has been used to establish the hydrophobicity of the anchored cavities and the polarity, so determined, lies in-between that of a 1:1 methanol-water mixture and pure methanol with the corresponding value of the dielectric constant around 55. Functionalization of the LDH has, therefore, resulted in the creation of hydrophobic nano-pockets within the essentially hydrophilic interlamellar space of the inorganic solid. It is shown here that neutral poly-aromatic hydrocarbons can be accommodated within these hydrophobic 'pockets'. Inclusion occurs by partitioning; the hydrophobic PAH guest molecule is driven from a polar solvent into the less polar interior of the anchored *b*-CD cavities (figure 11). The optical – absorption and emission – properties of the PAHs included within the functionalized Mg–Al LDH-CMCD solid are similar to that of dilute solutions of the PAH in non-polar solvents. This is not surprising since the included PAHs are prevented from aggregating by the fact that the *b*-CD cavities are anchored to the gallery walls. The uniqueness of these hybrid materials is that the optical properties of dilute solutions of the PAHs are realized in the solid state. Additionally, they are thermally stable over a wide temperature range. The emission properties of the PAHs included within the Mg–Al LDH-CMCD are not significantly altered even at elevated temperatures – temperatures normally at which even the PAH solids are not stable. In conclusion, we have demonstrated that neutral poly-aromatic hydrocarbons can be included within a cyclodextrin functionalized Mg–Al LDH. The new hybrid material combines the optical properties of the aromatic organic guest with the mechanical and thermal robustness of the inorganic solid host.

References

1. Whittingham M S 1982 *Intercalation chemistry* (New York: Academic Press)
2. Alberti G and Costantino U 1996 *Comprehensive supramolecular chemistry* (Chichester: Wiley) vol 7, p. 1
3. Gluech D S, Brough A R, Mountford P and Green M L H 1993 *Inorg. Chem.* **32** 1893
4. Aranda P and Hitzky R 1990 *Adv. Mater*. **2** 545
5. Jeevanandam P and Vasudevan S 1998 *Chem. Mater*. **10** 1276
6. Ogawa M and Kuroda K 1997 *Bull. Chem. Soc. Jpn.* **70** 2593
7. Venkataraman N V, Mohanambe L and Vasudevan S 2003 *J. Mater. Chem*. **13** 170
8. Venkataraman N V and Vasudevan S 2003 *J. Phys. Chem.* **B107** 5371
9. Wouter L and Pinnavaia T J 2001 *Green Chemistry* **3** 10
10. Venkataraman N V and Vasudevan S 2003 *J. Phys. Chem.* **B107** 10119
11. (a) Vogtle F 1991 *Supramolecular chemistry* (Chichester: Wiley); (b) Steed J W and Atwood J L 2000 *Supramolecular chemistry* (Chichester: Wiley)
12. Kijima T, Tanaka J, Goto M and Matsui Y 1984 *Nature* (*London*) **310** 45
13. Kijima T and Matsui Y 1986 *Nature* (*London*) **322** 533
14. (a) Zhao H and Vance G F 1997 *J. Chem. Soc., Dalton. Trans.* **11** 1961; (b) Zhao H and Vance G F 1998 *J. Inclusion Phenom.* **31** 305; (c) Zhao H and Vance G F 1998 *Clays Clay Miner.* **46** 712
15. Mohanambe L and Vasudevan S 2005 *Langmuir* **21** 10735
16. (a) Fujiki M, Deguchi T and Sanamesa I 1988 *Bull. Chem. Soc. Jpn.* **61** 1163; (b) Patonay G, Shapira A, Diamond P and Warner I M 1986 *J. Phys. Chem.* **90** 1963; (c) Shixiang G, Liansheng W, Qingguo H and Sukui H 1998 *Chemosphere* **37** 1299
17. Connors K A 1996 *Comprehensive supramolecular chemistry* (eds) J Szejtli J and T Osa (London: Pergamon) vol 3, p. 234
18. Khan I K and Hare D O 2002 *J. Mater. Chem.* **12** 3191
19. Constantino V R L and Pinnavaia T J 1995 *Inorg. Chem*. **34** 883
20. Miyata S 1977 *Clays. Clay. Miner.* **25** 14
21. Miyata S 1983 *Clays. Clay. Miner.* **31** 305
22. Miyata S 1975 *Clays. Clay. Miner*. **23** 369
23. De Roy A, Forano C, El Malki K and Bessi J P 1992 *Expanded clays and other microporous solids* (eds) M L Occelli and H E Robson (New York: Van Nostrand Reinhold) vol 2, p. 108
24. Cavani F, Trifiró F and Vaccari A 1991 *Catal. Today* **11** 173

25. Newman S and Jones W 1998 *New J. Chem*. **22** 105
26. Vaccari A 1999 *Appl. Clay Sci*. **14** 161
27. Rives V and Ulibarri M 1999 *Coord. Chem. Rev.* **181** 61
28. Choy J H, Kwak S Y, Park J S, Jeong Y J and Portier J 1999 *J. Am. Chem. Soc.* **121** 1399
29. Choy J H, Kwak S Y, Jeong Y J and Park J S 2000 *Angew. Chem., Int. Ed.* **39** 4042
30. Mohanambe L and Vasudevan S 2005 *Inorg. Chem.* **44** 2128
31. Mohanambe L and Vasudevan S 2005 *J. Phys. Chem.* **B109** 11865
32. Mohanambe L and Vasudevan S 2005 *J. Phys. Chem.* **B109** 22523
33. Mohanambe L and Vasudevan S 2004 *Inorg. Chem.* **43** 6421
34. Meyn M, Beneke K and Lagaly G 1990 *Inorg. Chem.* **29** 5201
35. Kalyanasundaram K and Thomas J K 1977 *J. Am. Chem. Soc.* **99** 2039
36. (a) Koyanagi M 1968 *J. Mol. Spectrosc*. **25** 273; (b) Robinson G W 1967 *J. Chem. Phys*. **46** 572
37. Valeur B 2001 *Molecular fluorescence: Principles and applications* (Weinheim, Berlin: Wiley-VCH Verlag)
38. Cary T C, Louis J P and Virgil H F 1979 *Science* **206** 831
39. Birks J B 1970 *Photophysics of aromatic molecules* (New York: John-Wiley and Sons)
40. Matsui K 1992 *Langmuir* **8** 673